

Lawrence Berkeley National Laboratory

LBL Publications

Title

Characterization of the Uranyl Ions with Humic Acids by X-Ray Absorption Spectroscopy

Permalink

<https://escholarship.org/uc/item/03c9j983>

Author

Reich, Tobias

Publication Date

1995-11-01



Lawrence Berkeley Laboratory

UNIVERSITY OF CALIFORNIA

CHEMICAL SCIENCES DIVISION

Presented at the American Chemical Society National Meeting,
Chicago, IL, August 20–24, 1995, and to be published in
Applications of Synchrotron Radiation in Industrial, Chemical,
and Materials Science Research

Characterization of the Interaction of Uranyl Ions with Humic Acids by X-Ray Absorption Spectroscopy

T. Reich, M.A. Denecke, S. Pompe, M. Bubner, K.H. Heise,
M. Schmidt, V. Brendler, L. Baraniak, H. Nitsche, P.G. Allen,
J.J. Bucher, N.M. Edelstein, and D.K. Shuh

November 1995



REFERENCE COPY
Does Not Circulate
Bldg. 50 Library.
Copy 1
LBL-38368

DISCLAIMER

This document was prepared as an account of work sponsored by the United States Government. While this document is believed to contain correct information, neither the United States Government nor any agency thereof, nor the Regents of the University of California, nor any of their employees, makes any warranty, express or implied, or assumes any legal responsibility for the accuracy, completeness, or usefulness of any information, apparatus, product, or process disclosed, or represents that its use would not infringe privately owned rights. Reference herein to any specific commercial product, process, or service by its trade name, trademark, manufacturer, or otherwise, does not necessarily constitute or imply its endorsement, recommendation, or favoring by the United States Government or any agency thereof, or the Regents of the University of California. The views and opinions of authors expressed herein do not necessarily state or reflect those of the United States Government or any agency thereof or the Regents of the University of California.

Characterization of the Interaction of Uranyl Ions with Humic Acids by X-Ray Absorption Spectroscopy

Tobias Reich,¹ Melissa A. Denecke,¹ Susanne Pompe,¹ Marianne Bubner,¹
Karl-Heinz Heise,¹ Maren Schmidt,¹ Vinzenz Brendler,¹ Lutz Baraniak,¹ Heino Nitsche,¹
Patrick G. Allen,² Jerome J. Bucher,² Norman M. Edelstein,² and David K. Shuh²

¹Forschungszentrum Rossendorf e.V., Institute of Radiochemistry, P.O. Box 510119
D-10314 Dresden, Germany

²Chemical Sciences Division, Ernest Orlando Lawrence Berkeley National Laboratory
University of California, Berkeley, California 94720

November 1995

This work was supported by the Institute of Radiochemistry, Forschungszentrum Rossendorf, Dresden, Germany, the Stanford Synchrotron Radiation Laboratory, and the Berkeley Lab, by the Director, Office of Energy Research, Office of Basic Energy Sciences, Chemical Sciences Division, of the U.S. Department of Energy, under Contract No. DE-AC03-76SF00098.

CHARACTERIZATION OF THE INTERACTION OF URANYL IONS WITH HUMIC ACIDS BY X-RAY ABSORPTION SPECTROSCOPY

Tobias Reich,¹ Melissa A. Denecke,¹
Susanne Pompe,¹ Marianne Bubner,¹ Karl-Heinz Heise,¹
Maren Schmidt,¹ Vinzenz Brendler,¹ Lutz Baraniak,¹ Heino Nitsche,¹
Patrick G. Allen,² Jerome J. Bucher,²
Norman M. Edelstein,² David K. Shuh²

¹Forschungszentrum Rossendorf e.V.
Institute of Radiochemistry,
P.O.Box 510119, D-01314 Dresden, Germany
²Lawrence Berkeley National Laboratory
Chemical Sciences Division
MS 70A-1150, Berkeley, CA 94720, USA

INTRODUCTION

Humic substances are present throughout the environment in soil and natural water. They are organic macromolecules with a variable structural formula, molecular weight, and a wide variety of functional groups depending on their origin. In natural waters, humic substances represent the main component of the "dissolved organic carbon" (DOC). The DOC may vary considerably from 1 mg/L at sea water surfaces to 50 mg/L at the surface in dark water swamps.¹ There is strong evidence that all actinides form complexes with humic substances in natural waters.² Therefore, humic substances can play an important role in the environmental migration of radionuclides by enhancing their transport. Retardation through humic substance interaction may be also possible due to formation of precipitating agglomerates. For remediation and restoration of contaminated environmental sites and risk assessment of future nuclear waste repositories, it is important to improve the predictive capabilities for radionuclide migration through a better understanding of the interaction of radionuclides with humic substances.

A large research program at the Institute of Radiochemistry at the Forschungszentrum Rossendorf is devoted to the study of the influence of humic acids (HA) on the environmental migration of uranium (VI) by a broad range of analytical and spectroscopic methods.³ The research is related to the environmental problems due to large uranium

mining and processing facilities in the Erzgebirge (Ore Mountains) which were operational in the Eastern part of Germany until 1990. Seepage waters from uranium mill tailing piles and from flooded mine shafts, which contain both uranium and humic substances, can act as a transport medium for the migration of uranium and its decay products into our environment.

By an operational definition, HA's are the part of humic substances which is soluble in alkaline and precipitating in acidic medium. The protolytic and complexation behavior of HA's is determined by their functional groups and substituents. The most important functional groups are carboxylic and phenolic OH groups. The amount of carboxylic and phenolic OH groups can vary considerably depending on the natural origin of the HA from 1.5-5.7 meq/g and 2.1-5.7 meq/g, respectively.⁴ Several phenomenological parameters, such as stability constant, complexing capacity, and loading capacity, quantitatively describe the complexation behavior of HA's with U(VI). For example, the following stability constants have been reported for the 1:1 and 1:2 complex of uranyl with HA at pH of 4.5 and ionic strength of 0.1: $\log \beta_1$ 5.16 and $\log \beta_2$ 9.31.⁵ The maximum amount of U(VI) that can be bound by HA at pH 4 is approximately 10-18% of its proton-exchange capacity (PEC).^{6,7}

It is important to describe the complexation behavior of HA not only on a phenomenological but also on a molecular level. Extended X-ray Absorption Fine Structure (EXAFS) analysis is a standard technique which can provide molecular-level information on the nearest-neighbor structure of a chosen absorbing atom.⁸ In the present study, EXAFS spectroscopy was applied to measure coordination numbers and distances of U(VI) to its nearest neighbors when it interacts with HA's. The molecular structure of HA's is so complex that only generic structural formulae are discussed in the literature (ca. Schulten et al.⁹). Therefore, our structural analysis of U(VI) interaction with HA's was based on the following strategy: 1) Investigation of solid and aqueous uranyl complexes with simple organic molecules which might represent "building blocks" of HA's. The goal is to identify certain structures of U(VI) complexes, such as chelate rings, monodentate, and bidentate configurations, depending on the presence of carboxylic and phenolic OH groups and their positions relative to each other in a given molecule. 2) Investigation of the U(VI) interaction with synthetic HA model substances. Synthetic HA is characterized by a chemical behavior similar to natural HA but with a considerably simpler overall structure.¹⁰ 3) Comparison of structural parameters obtained from U(VI) model systems with those where U(VI) interacted with HA's isolated from natural sources.

In the present paper, we report EXAFS studies of solid samples of uranyl acetate, salicylate, *o*-methoxybenzoate, and aqueous solutions of both uranyl acetate and malonate. The structural parameters are compared with those of uranyl humates which were prepared under various conditions from one synthetic and two natural HA's.

SAMPLE PREPARATION

Solid Uranyl Model Compounds

For uranyl acetate (sample A1), we used the commercially available uranyl acetate dihydrate (p.A., Merck) without further purification. Uranyl salicylate (sample A2) and uranyl o-methoxybenzoate (sample A3) were synthesized following a modified procedure used in Ref. 11. The last part of the synthesis was modified to yield anhydrous crystals. If no crystal water is present in the compound, the presence of an additional oxygen coordination in the equatorial uranyl shell can be excluded during the EXAFS analysis. Anhydrous bis(salicylato)dioxouranium(VI) was prepared by dissolving uranyl acetate dihydrate and salicylic acid with a molar ratio of 1:2 in ethanol at 65°C. Anhydrous bis(methoxybenzoato)dioxouranium(VI) was prepared in a similar manner by dissolving uranyl acetate dihydrate and o-methoxybenzoic acid in a molar proportion of 1:2 in ethanol at 60°C. For both cases, acetic acid and ethanol were separated from the mixture by lyophilization. The resulting products were dissolved in ethanol and concentrated again to remove the rest of acetic acid. Finally, the crystals were washed several times in benzene and freeze-dried. Elemental and thermal analysis (EA and TA) confirmed that the synthesis had resulted in a 1:2 uranyl salicylate and 1:2 uranyl mehtoxybenzoate without water of hydration.

Table 1. Sample composition and calculated speciation for model solutions of uranyl ions with acetic acid (Ac) and malonic acid (Mal).

	UO ₂ ²⁺ (mol/L)	Ligand (mol/L)	pH	I (mol/L)	Calculated speciation
B1	0.05	0.05 Ac	0.5	0.25	UO ₂ ²⁺ 100%
B2	0.05	0.2 Ac	2.9	0.5	UO ₂ ²⁺ 48%, UO ₂ Ac ⁺ 35%
B3	0.05	1.1 Ac	3.7	1.3	UO ₂ (Ac) ₂ ⁻ 100%
B4	0.05	0.2 Mal	4.0	1.05	UO ₂ Mal ₂ ²⁻ 100%

Aqueous Uranyl Model Solutions

Table 1 shows the molar ratio, pH, and ionic strength of the aqueous solutions of uranyl acetate (samples B1-B3) prepared. Solution B1 was prepared from a uranyl nitrate stock solution by adding acetic acid. Solutions B2 and B3 were made from uranyl acetate

dihydrate and acetic acid. The pH was adjusted by adding NaOH. For each solution the speciation was calculated by using the corresponding complex stability and acid dissociation constants,¹² the speciation modeling software EQ3/6,¹³ and the NEA Data Base.¹⁴ From the results of the calculation that are shown in Table 1, one can see that solution B1 contains only the hydrated uranyl species. Solution B2 is a mixture consisting predominantly of the hydrated uranyl ion and the 1:1 complex. The remaining 17% is a mixture of monomeric and dimeric hydroxyl species. Due to a large excess of acetic acid, solution B3 contains only the tris-acetato complex.

The concentration, pH, and ionic strength of a solution containing 100% of the 1:2 uranyl malonate complex (sample B4) is also given in Table 1. The solution was prepared from uranyl nitrate hexahydrate and malonic acid. The pH was adjusted by adding NaOH. The speciation was calculated similar to the uranyl acetate solutions with the corresponding constants for malonic acid and uranyl malonate.¹⁵

Uranyl Humates

Uranium (VI) was sorbed onto HA's by two different ways: Samples C1-C3 were prepared by shaking solid HA in a solution of uranyl nitrate or uranyl perchlorate for 45-50 hours. Samples D1-D5 are precipitates formed when uranyl solution was added to dissolved

Table 2. Sample preparation conditions for uranyl humates by sorption on solid HA (samples C) and precipitation out of HA solution (samples D).

	HA source	mg HA/mL soln.	pH	State	mg U/g HA
C1	Fluka	100	1	dry	100
C2	synthetic HA	400	<1	dry	176 (170)*
C3	Fluka (purified)	200	<1	dry	500 (185)*
D1	Aldrich	58	8-10	precip./soln.	92
D2	synthetic HA	173	5.1	precip./soln.	136
D3	synthetic HA	173	5.4	wet paste	137
D4	Fluka (purified)	125	5.3	wet paste	190
D5	Fluka (purified)	7.3	4	dry	540 (440)

* Uranium loading, given in parentheses, was determined by photospectrometric measurement of the uranyl concentration left in solution after separating the uranyl humate.

HA. We used three different HA's: Fluka HA (untreated and purified), Aldrich HA, and synthetic HA. Details of the purification of Fluka HA and of the synthesis of HA and their characterization by different analytical methods, e.g., elemental analysis, determination of functional groups, IR spectroscopy, and capillary electrophoresis, are given by Pompe et al.¹⁰ Table 2 summarizes the sample preparation conditions. Two sample preparations are described in detail below to illustrate the meaning of the columns in Table 2.

Sample C2 was prepared by shaking synthetic HA in a uranyl nitrate solution at a pH < 1 for 50 hours. The concentrations were 400 mg HA per mL solution and 176 mg U(VI) per gram HA (see columns 3 and 6 in Table 2). After centrifugation to separate the solid and liquid phases, the uranyl humate was washed several times with triply distilled water. For EXAFS measurements, the sample was dried by lyophilization (column 5 in Table 2). The U(VI) uptake by the HA was 170 mg/g (in parentheses in column 6 of Table 2) which corresponds to 97% of the total U(VI). The uranium uptake was measured only for a few selected samples.

To prepare sample D4, purified HA (Fluka) was first dissolved at pH 12. Then the pH was lowered to 5.7 with HClO₄. After adding 0.1 M acidic UO₂(ClO₄)₂ solution, the pH was adjusted to 5.3 by adding NaOH. The uranyl humate precipitated immediately upon adding the uranyl solution. The precipitate was separated from the solution by centrifugation and washed several times. This sample was measured by EXAFS as a wet paste.

EXPERIMENTAL

Uranium L_{III} edge X-ray absorption spectra (XAS) were measured at room temperature in transmission mode at the Stanford Synchrotron Radiation Laboratory (SSRL) on wiggler beamline 4-1 using a Si(220) double-crystal monochromator. Several samples were measured at the Hamburger Synchrotronstrahlungslabor (HASYLAB) using a Si(311) double-crystal monochromator at the bend magnet beamline RÖMO II. In order to obtain an energy calibration, the XAS spectrum of a solid uranyl nitrate hexahydrate sample was measured simultaneously. To reduce the higher-harmonic content of the X-ray beam at SSRL, the two Si crystals were detuned by 50%. For the EXAFS data analysis, we used the software package EXAFASPAK.¹⁶ Theoretical scattering amplitudes and phases were calculated with the program FEFF6.¹⁷ The threshold of the uranium L_{III} edge was set at 17185 eV. During the fit, a constant ΔE_0 shift of -13 eV was applied.

In the present work, structural analysis was restricted to the first two uranium coordination shells by fitting the Fourier-filtered EXAFS spectrum. Fourier filtering was performed to isolate the EXAFS contribution of the first two coordination shells from contributions of higher order shells which were observed for several samples. During the

fit, the coordination number of the axial oxygen atoms in the uranyl group, UO_2^{2+} , was kept constant at two. The remaining five parameters, e.g., coordination number, distances, and Debye-Waller (DW) factors, were allowed to vary. In a future publication, we will present a more detailed structural analysis of solid and aqueous model compounds where higher coordination shells and multiple scattering effects (see below) are included to fit the experimental EXAFS.

RESULTS AND DISCUSSION

Solid Uranyl Model Compounds

The experimental EXAFS spectra of samples A1-A3 and their corresponding Fourier transforms (FT) are shown in Fig. 1. The structural parameters for the first two uranium coordination shells obtained from the fit are presented in Table 3.

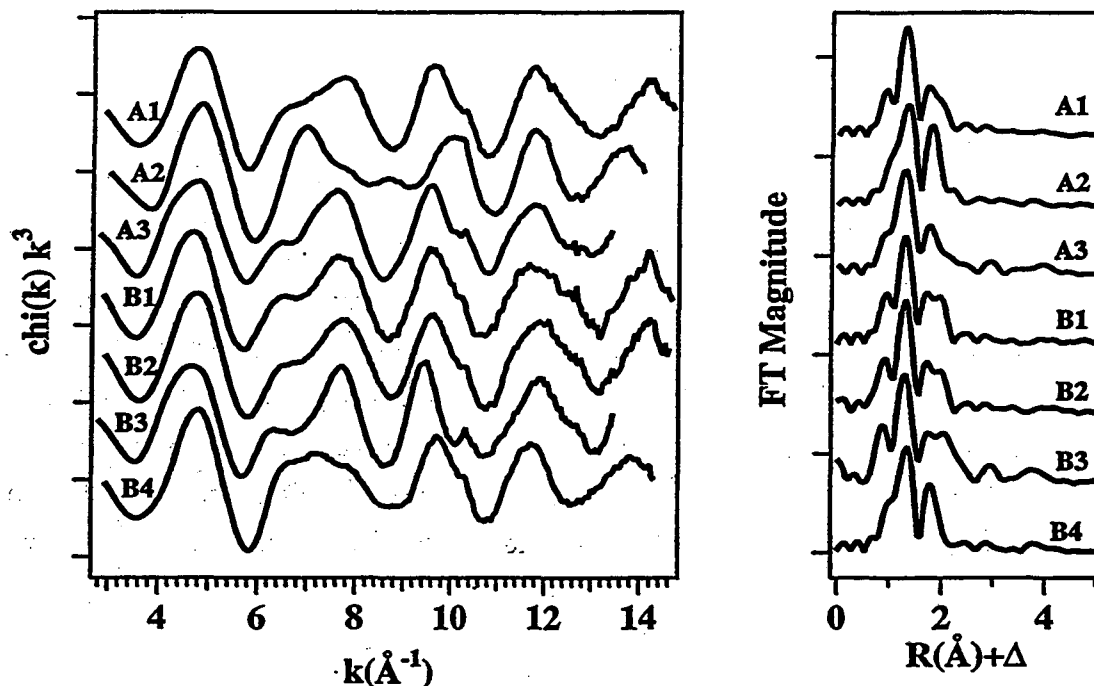


Fig. 1. Left panel: Experimental U L_{III} edge EXAFS of samples A1 - B4. Right panel: Fourier-transformed EXAFS of samples A1 - B4.

The crystal structure of uranyl acetate dihydrate has been determined by single-crystal X-ray diffraction (XRD).¹⁸ The bond lengths between uranium and the two axial oxygen atoms are 1.74 Å and 1.76 Å. The equatorial plane of the uranyl group contains five oxygen atoms: one oxygen at 2.34 Å from a water molecule, two oxygen atoms at 2.37 Å from two different bidentate bridging acetate groups, and two oxygen atoms at 2.45 Å from a chelating acetate group. As shown in Table 3, the uranium-oxygen bond distances agree within ± 0.02 Å with the weighted average distances measured by XRD. Due to the limited data range in k space, the different bond lengths of the equatorial oxygen atoms are not resolved by EXAFS. The broader distribution of U-O_{eq} distances is indicated by a larger DW factor of the equatorial shell as compared to the axial shell. A coordination number of 4.8($\pm 15\%$) for the equatorial shell agrees nicely with the crystal structure. Based on the agreement of structural parameters obtained by EXAFS and XRD, we conclude that theoretical scattering phases and amplitudes calculated by FEFF can be used to fit the EXAFS of organic uranyl complexes of unknown structure.

The experimental EXAFS curve of uranyl salicylate (sample A2) differs from that of uranyl acetate (see Fig. 1). The fit shows that the equatorial coordination of the uranyl group consists of approximately four oxygen atoms at a distance of 2.32 Å. The U-O_{eq} bond distance has a narrow distribution as indicated by the small DW factor of 0.003 (see Table 3). For a discussion of possible uranyl salicylate structures, it is essential to include information obtained by other analytical techniques. TA and EA measurements suggest that

Table 3. EXAFS structural parameters for the first two uranium coordination shells in solid uranyl model compounds and uranyl model solutions.

Sample	U-O _{ax}			U-O _{eq}		
	N	R(Å)	$\sigma^2(\text{Å}^2)$	N	R(Å)	$\sigma^2(\text{Å}^2)$
A1 (Uranyl acetate)	2	1.77	0.003	4.8(4)*	2.41	0.007
A2 (Uranyl salicylate)	2	1.78	0.003	3.6(2)	2.32	0.003
A3 (Uranyl methoxybenzoate)	2	1.78	0.002	4.3(5)	2.44	0.010
B1 (UO ₂ ²⁺ 100%)	2	1.77	0.002	4.8(3)	2.42	0.007
B2 (UO ₂ ²⁺ 48%, UO ₂ Ac ⁺ 35%)	2	1.77	0.002	4.9(5)	2.40	0.008
B3 (UO ₂ (Ac) ₂ ⁻ 100%)	2	1.78	0.002	4.7(5)	2.46	0.006
B4 (UO ₂ Mal ₂ ²⁻ 100%)	2	1.79	0.002	4.6(3)	2.37	0.007

*) Uncertainties, given in parentheses, are statistical errors and do not reflect possible systematic errors.

the uranyl ion forms an anhydrous bis-salicylato complex. The coordination of uranium with a water molecule, as in the case of uranyl acetate, can be ruled out. The IR spectra of uranyl salicylate did not show evidence of free phenolic OH groups as in the case of salicylic acid. Therefore, it can be concluded that the phenolic OH group of salicylic acid participates in the uranyl complexation. Together with the carboxylic OH group, a six-member chelate ring can be formed in the equatorial plane by each of the two salicylato molecules surrounding the uranium atom.

In o-methoxybenzoic acid the phenolic OH group is replaced by a methyl group and can not participate in the complex formation. By comparing the EXAFS spectra of uranyl salicylate and uranyl methoxybenzoate given in Fig. 1, it can be seen that the two uranyl complexes have different structures. The fit reveals that the complexes A2 and A3 differ in their U-O bond length and DW factor of the equatorial uranium shell. An average U-O_{eq} bond distance of 2.44 Å is close to that of the chelating acetate group of sample A1. Sample A3 in Fig. 1 shows pronounced peaks at 2.8 Å and 3.7 Å in the FT (uncorrected for EXAFS phase shifts). Similar peaks have been reported recently in an EXAFS study of monomeric tris-carbonato and trimeric bis-carbonato complexes with U(VI).¹⁹ It was shown that multiple scattering pathways within the uranyl group and along the linear U-C-O configuration contribute significantly to the EXAFS FT peaks centered at 3.0 Å and 3.6 Å, respectively. If a similar explanation is valid for sample A3, the terminal carbon of the carboxylic group can give rise to the peak at 3.7 Å originating from multiple scattering along the linear U-C-C configuration. The large DW factor for the equatorial oxygen bond distance indicates a broad distribution. This may result from the presence of a bridging configuration of the carboxylic group.

Aqueous Uranyl Model Solutions

According to the calculated speciation described above, uranyl ions in solution B1 are coordinated by water molecules. At a pH of 0.5, ligands such as nitrate, chloride, perchlorate, and acetic acid do not coordinate uranium in a 0.05 M uranyl solution. The best fit of the Fourier-filtered EXAFS is obtained with five oxygen atoms at 2.42 Å, forming the second uranium coordination shell. Similar structural parameters as those listed for sample B1 in Table 3 have been obtained for other uranyl solutions at very low pH. For example, the U-O distances in a 10⁻³ M UO₂Cl₂ solution in 1.2x10⁻² M HCl are 1.78 Å and 2.41 Å, respectively.²⁰ In a 0.05 M uranyl nitrate solution at pH 1.8, two U-O coordination shells at distances of 1.77 Å and 2.40 Å were observed.²¹

Due to a higher pH and the larger acetate concentration of sample B2 compared to sample B1, solution B2 should contain the uranyl complex with a 1:1 molar ratio in addition to the hydrated uranyl ion. The measured EXAFS spectrum given in Fig. 1 represents a

superposition of all uranyl species present in the solution. As can be seen from Table 3, the nearest-neighbor structure of U(VI) in solutions B1 and B2 is the same within the experimental error. If there is any 1:1 complex present in solution B2, it is either undetectable by EXAFS or exhibits similar structural parameters as $\text{UO}_2(\text{H}_2\text{O})_5^{2+}$.

Based on thermodynamic data, the tris-acetato complex is the only uranyl species present in solution B3. The EXAFS spectrum of solution B3 differs from those of samples B1 and B2, especially in the 6-10 \AA^{-1} region (see Fig. 1). The fit of the Fourier-filtered EXAFS shows an expansion of the equatorial U-O bond by 0.05 \AA compared to samples B1 and B2. The value of 2.46 \AA is close to the value of 2.45 \AA for the chelating carboxylic carbon in solid uranyl acetate. Therefore, it is very likely that the carboxylic groups coordinate as bidentates. In a bidentate configuration, carboxylic carbon and methyl carbon at 2.8 \AA and 4.34 \AA should be observable by EXAFS, respectively.

The EXAFS spectrum of sample B4 with a 1:2 molar ratio of uranyl to malonic acid is different from those of the other model solutions, as shown in Fig. 1. A two-shell fit of the Fourier-filtered EXAFS gives a slightly longer axial U-O bond of 1.79 \AA and a significantly contracted equatorial U-O bond of 2.37 \AA compared to solutions B1-B3. The equatorial bond length matches that of a bridging acetic carbon rather than a chelating acetic carbon in solid uranyl acetate dihydrate. This leads to the conclusion that the carboxylic OH groups form a monodentate configuration with the uranyl ion. Note that the FT of sample B4 does not exhibit a pronounced peak at 3.8 \AA , as in the case of samples A3 and B3, where chelating carboxylic groups are presumed to dominate the uranium coordination in the equatorial plane. This conclusion also agrees with structures proposed in the literature where the terminal carboxylic groups of two malonic acid molecules form two six-member rings in the equatorial plane of the uranyl group.²²

Uranyl Humates

Inspection of the EXAFS spectra of uranyl humates given in Fig. 2, one notices that all samples have similar EXAFS except for sample D1 which differs in phase in the 6-11 \AA^{-1} range. This situation is more clearly reflected in the structural parameters for the first two uranium coordination shells given in Table 4. Fig. 3 shows the Fourier-filtered EXAFS, the corresponding FT's, and the best fit for the two uranyl humate samples.

The structural parameters of samples C1-C3 and D2-D5 are the same to within the error inherent to EXAFS analysis and can be summarized as follows: The U-O distance to the axial oxygen atoms averages 1.78(2) \AA with a DW factor of 0.002 \AA^2 ; and the equatorial shell consists of approximately 5 oxygen atoms at 2.38(2) \AA with a DW factor of 0.013(3) \AA^2 . In sample D1 the bond distance U-O_{eq} of 2.30 \AA is much shorter. The longer U-O_{ax} bond of 1.83 \AA is explained by the roughly inverse relationship between the electron density

along the axial and equatorial U-O bonds. The agreement of the nearest-neighbor structure of U(VI) when it interacts with both Fluka HA and the synthetic HA can be interpreted as a success of the synthesis. Although the synthetic HA differs in its molecular structure and number of functional groups from the natural HA, it shows identical functionality with respect to interaction with uranyl ions. This is a somewhat surprising result if one considers that the uranyl humate samples were prepared from different HA starting materials at different pH and measured as wet pastes or dried powders. How can this be explained and why has one sample different structural parameters?

The main difference between sample D1 and the other uranyl humates is that D1 was prepared at high pH and with a uranium concentration that accounted for the loading capacity of dissolved HA. The amount of uranyl ions to prepare D1 at pH 8-10 was 15% of the measured PEC at pH of 4. Due to the increased deprotonation of the carboxylic and phenolic OH groups at higher pH, the actual loading capacity of the HA may be even higher than 15%.

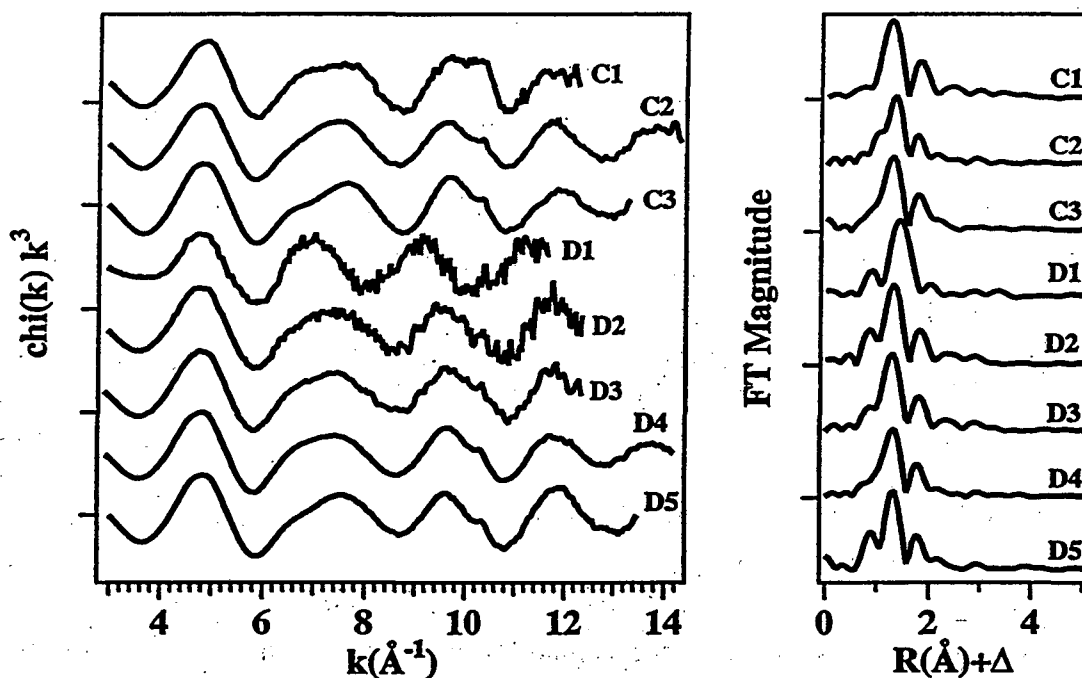


Fig. 2. Left panel: Experimental U L_{III} edge EXAFS of samples C1 - D5. Right panel: Fourier-transformed EXAFS of samples C1 - D5.

Table 4. EXAFS structural parameters for the first two uranium coordination shells in uranyl humates.

Sample name	U-O _{ax}			U-O _{eq}		
	N	R(Å)	$\sigma^2(\text{Å}^2)$	N	R(Å)	$\sigma^2(\text{Å}^2)$
C1	2	1.77	0.002	4.5(6)*	2.37	0.010
C2	2	1.78	0.002	5.2(6)	2.38	0.014
C3	2	1.77	0.002	5.0(5)	2.39	0.010
D1	2	1.83	0.002	4.6(7)	2.30	0.015
D2	2	1.79	0.002	4.5(7)	2.38	0.012
D3	2	1.78	0.002	5.0(6)	2.38	0.012
D4	2	1.78	0.002	4.8(5)	2.38	0.011
D5	2	1.78	0.002	5.2(8)	2.37	0.013

* Uncertainties, given in parentheses, are statistical errors and do not reflect possible systematic errors.

For samples C1-C3, which were prepared at $\text{pH} \leq 1$, fewer functional groups will deprotonate and can complex with uranyl ions. Additionally, the uranyl concentration in solution relative to the HA's PEC at pH 4 exceeded the 15-18% level for samples C1-C3 and D2-D5. For example, the PEC of purified HA (Fluka) was defined by the total number of COOH and phenolic OH groups and was measured to be 8.5 meq/g.¹⁰ The amount of U(VI) during the preparation of sample D5 corresponds to 53% of its PEC. The measured uptake of U(VI) by the HA was 43% (Table 2). High levels of uranium uptake are possible as a result of sorption on non-specific sites in addition to site-specific sorption onto certain functional groups. The EXAFS spectra of such samples represent a superposition of uranium atoms sorbed onto different specific and non-specific sites. For the case of sample D1, the amount of U(VI) was below the saturation level of the specific sorption sites. A similar short U-O_{eq} distance as observed for sample D1 was measured only for solid uranyl salicylate. A comparison with other solid and aqueous uranyl model complexes leads to the conclusion, that the phenolic OH groups in sample D1 participate in the uranyl humate interaction and cause the observed short U-O bond of 2.30 Å.

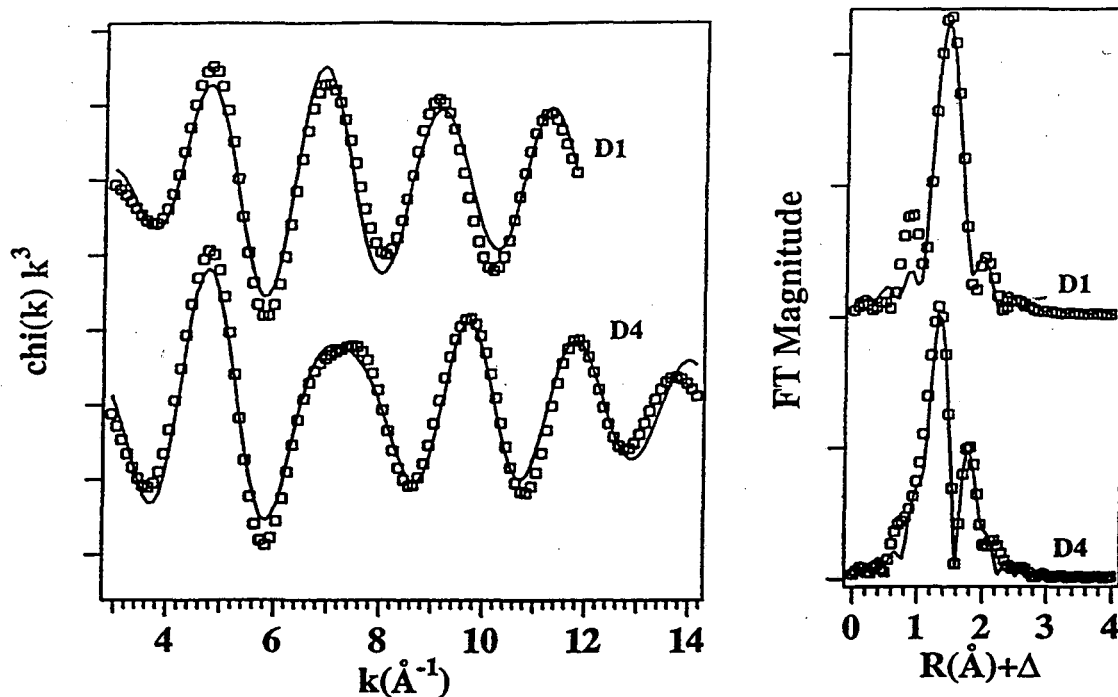


Fig. 3. Left panel: Fourier-filtered (squares) and fitted (solid line) U L_{III} edge EXAFS of samples D1 and D4. Right panel: Fourier-transformed EXAFS of samples D1 - D4. Squares - Fourier-filtered data; solid line - fit.

Clearly, such a conclusion has to be supported by additional measurements of humate samples with uranium concentrations below the loading capacity of the HA to avoid sorption on non-specific sites. This will be a challenging experiment due to the large number of different functional groups of the HA's. One possibility is to block phenolic OH groups of the HA by derivatization with diazomethane.¹⁰ Carboxylic COOH and phenolic OH groups can be derivatized into COOCH₃ and OCH₃ groups, respectively. In a second reaction with alkali, the carboxylic esters can be specifically hydrolyzed. Therefore, the OCH₃ groups will remain unchanged and cannot interact with uranyl ions similar to the o-methoxybenzoic acid described herein.

SUMMARY

Humic acids can play an important role in the transport properties of radionuclides throughout our environment. A molecular-level understanding of the structures formed as a result of the interaction of radionuclides with HA's is essential for the description of the complexation behavior of radionuclides. The complexation of HA's mainly occurs through their carboxylic and phenolic OH groups. In the present work, we obtained EXAFS

structural parameters for the nearest-neighbors environment of U(VI) in uranyl humates. The influence of carboxylic and phenolic OH groups on the structure of uranyl complexes was also studied by measuring the EXAFS of selected simple model compounds in solid and liquid phases.

Uranyl acetate, uranyl salicylate, and uranyl o-methoxybenzoate were selected as solid model compounds and studied by EXAFS. From previous XRD analysis it is known that in uranyl acetate dihydrate the carboxylic group coordinates with the uranium in two ways with different U-O distances. For the bridging carboxylic group, the U-O_{eq} bond distance is 2.37 Å. For the chelating carboxylic group, the U-O_{eq} bond is 0.08 Å longer than for the bridging configuration. The agreement between the structural parameters obtained by EXAFS and XRD confirmed the conclusion of earlier EXAFS studies of uranyl compounds that theoretical scattering amplitudes and phases calculated by FEFF can be used successfully in the U L_{III} edge EXAFS analysis.²³

We are not aware of any XRD studies of crystalline anhydrous bis-(salicylato) dioxouranium(VI) and anhydrous bis-(methoxybenzoato) dioxouranium(VI). These two model compounds were measured with EXAFS to study structural changes of the uranyl complex when the phenolic OH group is replaced by OCH₃. In addition, the configuration of a COOH group and a phenolic OH group in ortho position to each other is often considered as an important structural element of HA's. In uranyl salicylate, approximately four short U-O_{eq} bonds were observed at 2.32 Å. By replacing the phenolic OH group of salicylic acid by OCH₃, the structure of the resulting uranyl complex changes significantly as indicated by an increase of the U-O_{eq} bond length by 0.12 Å. Based on the EXAFS and IR spectroscopic data, the structure of the uranyl bis-salicylato complex is dominated by the formation of six-member chelate rings involving the carboxylic and phenolic OH groups. The uranyl bis-methoxybenzoato complex is characterized by a bidentate configuration of the carboxylic oxygen atoms.

EXAFS is a valuable tool for structural analysis especially of amorphous systems. Structural parameters of several uranyl species in aqueous solutions with acetic and malonic acids were determined by EXAFS. For EXAFS measurements it is important to prepare samples which contain only one uranyl species. If several species are present simultaneously, the resulting average EXAFS signal may be difficult if not impossible to interpret. Therefore, prior to the preparation of the uranyl solutions, the appropriate conditions, e.g., metal and ligand concentrations and pH, were calculated based on thermodynamic data. For both solid and aqueous uranyl model systems, the bond distance of uranium to the equatorial oxygen atoms is most sensitive to differences in the coordination. A short U-O distance of 2.37 Å is observed for end-on coordination of the carboxylic group of the bis-malonato complex. For chelating bidentate coordination of the carboxylic group in the case of the uranyl tris-acetato complex, the U-O bond length is

approximately 0.07 Å longer. A medium U-O bond distance of 2.41 Å is observed for the $\text{UO}_2(\text{H}_2\text{O})_5^{2+}$ species.

HA's are characterized by a complicated structure and one could expect that the EXAFS signal of different HA's would look similar due to averaging over the large number of functional groups. Out of eight samples studied by EXAFS, seven uranyl humates exhibit similar structural parameters. Under the chosen sample preparation conditions, no difference was observed between dried powders and wet pastes and natural and synthetic HA's. Only one uranyl humate sample (D1) exhibits significant different axial and equatorial U-O bond lengths. Although the interpretation of this result is limited by the number of samples studied, this difference is discussed in terms of uranyl sorption on specific and non-specific sites depending on proton exchange capacity and loading capacity of the HA's, and the pH and uranium concentration during the sample preparation. For the majority of uranyl humates, the structural parameters represent an average over uranyl sorbed on specific and non-specific sites. Based on the comparison of structural parameters observed in solid and aqueous uranyl model compounds, the short U-O_{eq} bond distance in sample D1 is interpreted as site specific sorption involving phenolic OH groups. This preliminary conclusion needs to be supported further by systematic EXAFS experiments on a series of uranyl humates prepared from chemically modified HA's to block certain functional groups and with lower uranium concentrations in solution.

In summary, pronounced changes observed in the equatorial uranyl coordination of organic uranyl model compounds and uranyl humates as a function of the uranyl speciation is encouraging for further EXAFS studies to obtain a better molecular-level understanding of the uranyl humate interaction. For certain complex configurations, e.g., chelating carboxylic groups, the amount of structural information will be enhanced further by including more distant coordination shells and multiple scattering effects in the EXAFS analysis.

ACKNOWLEDGMENT

We thank M. Meyer, R. Nicolai, R. Ruske, and G. Schuster for their valuable help in the sample preparation and characterization. EXAFS measurements were performed in part at SSRL, which is operated by the U.S. Department of Energy, Office of Basic Energy Sciences, Division of Chemical Sciences.

REFERENCES

- (1) Leenher, J. A.; Malcolm, R. C.; McKinley, P. W.; Eccoles, L. A. *J. Res. U.S. Geol. Survey* **1974**, *2*, 361-369.

- (2) Choppin, G. R.; Allard, B. In *Handbook of Physics and Chemistry of the Actinides Vol. 3*; A. J. Freeman and C. Keller, Eds.; North Holland: 1985.
- (3) Nitsche, H. "Institute of Radiochemistry, Annual Report 1994" Forschungszentrum Rossendorf e.V., Dresden, Germany, 1995.
- (4) Grauer, R. "Zur Koordinationschemie der Huminstoffe, Report No. 24," Paul Scherrer Institut, 1989.
- (5) Munier-Lamy, C. *Organic Geochim.* 1986, 9, 285.
- (6) Czerwinski, K. R.; Buckau, G.; Scherbaum, F.; Kim, J. I. *Radiochim. Acta* 1994, 65, 111-119.
- (7) Schmidt, M.; Baraniak, L.; Bernhard, G.; Nitsche, H. In *Institute of Radiochemistry, Annual Report 1994*; H. Nitsche, Ed.; Forschungszentrum Rossendorf e.V.: Dresden, Germany, 1995; pp 58-59.
- (8) Koningsberger, D. C.; Prins, R. *X-Ray Absorption: Principles, Applications, Techniques of EXAFS, SEXAFS and XANES*; John Wiley & Sons: New York, 1988.
- (9) Schulten, H. R.; Schnitzer, M. *Naturwissenschaften* 1993, 80, 29-30.
- (10) Pompe, S.; Bubner, M.; Brachmann, A.; Geipel, G.; Reich, T.; Denecke, M. A.; Nicolai, R.; Heise, K. H.; Nitsche, H. *Radiochim. Acta* 1995, submitted.
- (11) Kim, B.-I.; Miyake, C.; Imoto, S. *J. Inorg. Nucl. Chem.* 1974, 36, 2015-2021.
- (12) Rabinowitch, E.; Belford, R. L. *Spectroscopy and Photochemistry of Uranyl Compounds*; Pergamon Press: New York, 1964, pp 125.
- (13) Wolery, T. J. "EQ3/6, A Software Package for the Geochemical Modeling of Aqueous Systems," Lawrence Livermore National Laboratory, Livermore, CA, USA, 1992.
- (14) OECD Nuclear Energy Agency. *Thermodynamic Data Base. Chemical Thermodynamics of Uranium*; Elsevier: Amsterdam, 1992.
- (15) Paramonova, V. I.; Mesewitsch, A. N.; Tsi-Guan, M. A. *Radiokhimiya* 1964, 11, 682-694.
- (16) George, G. N.; Pickering, I. J. "EXAFSPAK: A Suite of Computer Programs for Analysis of X-ray Absorption Spectra," Stanford Synchrotron Radiation Laboratory, Stanford, CA, USA, 1995.
- (17) Mustre de Leon, J.; Rehr, J. J.; Zabinsky, S. I.; Albers, R. C. *Phys. Rev. B* 1991, 44, 4146-4156.
- (18) Howatson, J.; Grev, D. M. *J. Inorg. Nucl. Chem.* 1975, 37, 1933-1935.
- (19) Allen, P. G.; Bucher, J. J.; Clark, D. L.; Edelstein, N. M.; Ekberg, S. A.; Gohdes, J. W.; Hudson, E. A.; Kaltsoyannis, N.; Lukens, W. W.; Neu, M. P.; Palmer, P. D.; Reich, T.; Shuh, D. K.; Tait, C. D.; Zwick, B. D. *Inorg. Chem.* 1995, 34, 4797-4807.
- (20) Hudson, E. A.; Terminello, L. J.; Viani, B. E.; Reich, T.; Bucher, J. J.; Shuh, D. K.; Edelstein, N. M. In *Application of Synchrotron Radiation Techniques to Materials Science: MRS Symposium Proceedings, Vol 375*; D. L. Perry, N. D. Shinn, K. L. D'Amico, G. Ice and L. J. Terminello, Eds.; Materials Research Society: Pittsburgh, 1995; pp 235.
- (21) Dent, A. J.; Ramsay, J. D. F.; Swanton, S. W. *J. Colloid Interface Sci.* 1992, 150, 45-60.
- (22) Rajan, K. S.; Martell, A. E. *J. Inorg. Nucl. Chem.* 1967, 29, 523-529.
- (23) Thompson, H. A.; Brown, G. E.; Parks, G. A. *Physica B* 1995, 208/209, 167-168.

LAWRENCE BERKELEY NATIONAL LABORATORY
UNIVERSITY OF CALIFORNIA
TECHNICAL & ELECTRONIC INFORMATION DEPARTMENT
BERKELEY, CALIFORNIA 94720